Ramshaw, C., "Secondary Nucleation in Mechanically Agitated Crystallizers: Crystal Motion in the Impeller Region," *The Chemical Engineer*, No. 287/8, 446 (1974).
Randolph, A. D., M. A. Larson, *Theory of Particulate Processes*, Academic Press, New York (1971).
Randolph, A. D., M. D. Cise, "Nucleation Kinetics of the Potassium Sulphate-Water System," *AIChE J.*, 18, 798 (1972).
Rusli, I. T., "Origin, Size Distribution and Growth of Small Crystals in Contact Nucleation," M.S. thesis, Chemical Engineering Department, Iowa State University (1978).
van't Land, C. M., B. G. Wienk, "Control of Particle Size in Industrial NaCl Crystallization," in *Industrial Crystallization*, p. 51, Plenum Press, New York (1976).
Youngquist, G. R., A. D. Randolph, "Secondary Nucleation in a Class II System: Ammonium Sulphate-Water," *AIChE J.*, 18, 421 (1972).

Manuscript received August 3, 1978; revision received May 4, and accepted May 7, 1979.

Heat Transfer with Stratified Gas-Liquid Flow

E. JAMES DAVIS
NICHOLAS P. CHEREMISINOFF
and
CHRISTOPHER J. GUZY

Department of Chemical Engineering
Clarkson College of Technology
Potsdam, New York 13676

This article presents a method for predicting local Nusselt numbers for heat transfer to a stratified gas-liquid flow for turbulent liquid/turbulent gas conditions. A mathematical model based on the analogy between momentum transfer and heat transfer is developed and tested, using heat transfer and fluid mechanics data taken for air/water flow in a 63.5 mm I.D. tube. The fluid mechanics parameters required for the prediction of the heat transfer characteristics are obtained in the manner outlined elsewhere. Liquid phase Nusselt numbers predicted by the analogy are shown to be in agreement with experimental results for large and small amplitude wavy interfacial conditions. The circumferential average gas phase Nusselt numbers are in rough agreement with the Dittus-Boelter equation for single phase flow based on flow through a conduit of irregular shape. There is a tendency for the average gas phase Nusselt numbers to scatter about predicted values because of the effects of splashing and droplet deposition on the tube wall in the vicinity of the gas-liquid interface.

SCOPE

Two-phase gas-liquid flow with heat transfer occurs in a variety of process equipment, including feed preheaters for gas-liquid reactors, cooler/condensers, reboilers, evaporators and distillation equipment. Horizontal stratified flows occurring in heat exchange equipment involve heat transfer to both phases, and the prediction of the heat transfer characteristics is complicated by the existence of interfacial waves and droplet formation at higher gas and liquid flow rates. Depending on the flow rates, small amplitude capillary waves or large amplitude roll waves occur, and when the gas flow rate is sufficiently high, significant droplet entrainment occurs—to further complicate the heat transfer process.

In this article, we analyze and support by experimental data, the transfer of heat to a turbulent/turbulent stratified flow in a horizontal pipe. Fluid flow characteristics of stratified gas-liquid flows are now reasonably predictable due, to the studies of Yu and Sparrow (1967) on laminar/laminar flows, of Etchells (1970), Govier and Aziz (1972), Agarwal et al. (1973) and Russell et al. (1974) on laminar liquid/turbulent gas flows and of Cheremisinoff and Davis (1979) in a companion paper on turbulent/turbulent flows. But considerably less work of a fundamental nature has been done on the heat transfer characteristics of such flows. Rosson and Myers (1965) and Davis (1975) had considerable success in applying the von Karman analogy to gas-liquid flow heat transfer, and we extend these concepts and test the analysis with new data for air/water flow.

CONCLUSIONS AND SIGNIFICANCE

An analogy between momentum transfer and heat transfer can be applied to predict the heat transfer characteristics of the liquid layer of a stratified gas-liquid flow, even when appreciable wave action occurs at the gas-liquid interface. Using wall shear stresses predicted by the method outlined in a companion paper and using the geometric model of that paper, we predict liquid phase Nusselt numbers within 20% of measured values over a fairly wide range of flow rates and interfacial conditions. Even when some droplet entrainment occurs, our analysis agrees with experiments, but such agreement cannot be expected to hold at high gas flow rates, for which an appreciable fraction of the liquid is entrained.

Current address for Davis and Guzy: Department of Chemical and Nuclear Engineering, University of New Mexico, Albuquerque, NM 87131.

0065-8812-79-3055-0958-$01.05.

Gas phase Nusselt numbers for the various interfacial conditions can be predicted with fair accuracy from the Dittus-Boelter equation, using the Reynolds number based on the cross-sectional area occupied by the gas phase. Results for small-amplitude wavy interfaces are in good agreement with the Dittus-Boelter equation, but for roll wave conditions and when entrainment occurs, the scatter is great, owing to splashing and droplet deposition. Local Nusselt numbers for the gas phase vary appreciably around the periphery of the gas phase region, attaining a minimum at the top of the tube.

Using the companion paper by Cheremisinoff and Davis (1979) to predict the fluid flow parameters and the momentum and heat transfer analogy of this paper, the heat transfer characteristics of stratified turbulent/turbulent gas-liquid flows can be predicted from gross information on the pipe size, gas and liquid flow rates and physical properties.

Analogies between momentum transfer and heat transfer with turbulent flow fields have been used for decades for single phase flow, and Dukler (1959) and Hewitt (1961) successfully applied them to the liquid phase for vertical annular two-phase gas-liquid flows. Using eddy viscosity expressions developed for single phase flow, they determined the temperature profile in the liquid phase by applying the analogy between the momentum flux, τ, and heat flux, q, which is summarized by the equation,

$$\frac{q}{\tau} = C_P \left[\frac{(\nu/Pr) + (\epsilon_M/Pr_t)}{\nu + \epsilon_M} \right] \frac{dT}{du} \qquad (1)$$

where the turbulent Prandtl number is defined by $Pr_t = \epsilon_M/\epsilon_H$. Dukler and Hewitt used Deissler's (1959) expression for the eddy viscosity, ϵ_M, in the laminar sublayer and buffer zone of the turbulent flow field and von Karman's (1939) expression for the turbulent core.

Rosson and Myers (1965) applied the von Karman analogy, which treats only the laminar sublayer and buffer zone by means of the universal velocity profile for turbulent flow (u^+ as a function of y^+), to predict condensing coefficients for condensation in a horizontal pipe. Although their comparison between analysis and experimental data shows a great deal of scatter, the analogy appears to be valid for the stratified flow regime encountered.

Davis et al. (1975) applied the von Karman analogy to heat transfer with wavy stratified flow in a rectangular channel of large aspect ratio (width to height ratio of 10:1). Theirs was a more rigorous test of the analogy, because the liquid layer thickness and other fluid mechanics parameters were measured directly. The Nusselt numbers predicted by means of the analogy were found to be in good agreement with wavy liquid film flow in both the small-amplitude wave and roll wave regimes. Furthermore, Davis et al. (1977) showed that the interfacial wave structure encountered with stratified and annular flows in a circular tube is similar to that measured using the parallel plate (rectangular channel) configuration, so it is anticipated that the heat transfer characteristics should be similar.

It is the purpose of this article to show that the analogy proposed by Dukler (1959) can be extended to wavy stratified flows in horizontal circular tubes and that the analysis can be incorporated in a design procedure for the prediction of the heat transfer characteristics of two-phase stratified gas-liquid flow.

ANALYSIS OF THE LIQUID PHASE

Consider the flow cross section and geometric parameters of Figure 1. The gas-liquid interface is taken to be the average position of the liquid level, and the geometric parameters are related by the following equations:

$$y_0/D = (1 - \cos\gamma/2)/2 \qquad (2)$$

$$w_i/D = 2[(y_0/D) - (y_0/D)^2]^{1/2} \qquad (3)$$

$$R_L = A_L/A = (\gamma - \sin\gamma)/2\pi \qquad (4)$$

$$R_G = A_G/A = 1 - R_L \qquad (5)$$

$$p_L/p = \gamma/2\pi = 1 - p_G/p \qquad (6)$$

$$D_{EL}/D = 4A_L/p_L D = R_L/(p_L/p) \qquad (7)$$

$$D_{EG}/D = 4A_G/(p_G + w_i)D = R_G/[(p_G/p) + (w_i/\pi D)] \qquad (8)$$

The equivalent diameter for the liquid layer excludes the perimeter of the interface by convention, and this definition is consistent with the analysis of Cheremisinoff and Davis (1979).

Since the gas-liquid interface associated with turbulent/turbulent flow is not usually smooth, we shall consider y_0 to be the time-average distance from the bottom of the pipe to the interface on a vertical plane through the tube centerline. The mathematical model of the fluid mechanics developed by Cheremisinoff and Davis (1979) applies here, and we shall not repeat the details.

For the turbulent liquid layer the heat flux can be written as

$$q = -C_{LP_L}(\alpha + \epsilon_H)\frac{dT}{dy} \qquad (9)$$

where y is the distance from the tube wall in the direction of the inward normal to the wall, and ϵ_H is the eddy thermal conductivity, which we shall assume to equal the eddy viscosity, ϵ_M. That is, we consider the turbulent Prandtl number defined by $Pr_t = \epsilon_M/\epsilon_H$ to be unity, a result consistent with the results of Davis, Hung and Arciero (1975) and Davis, Cheremisinoff and Sambasivan (1977) for heat transfer to the liquid layer for stratified air/water and air/glycerol solution flows.

The development of the equations for the temperature field in the turbulent liquid is similar to that described

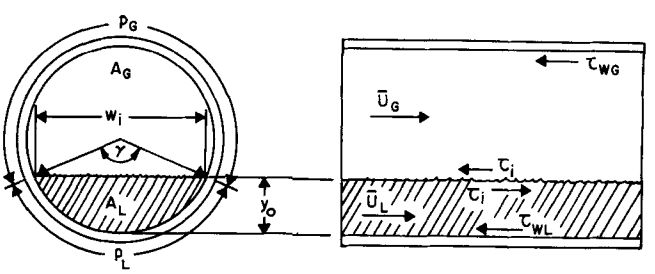

Figure 1. The flow system under consideration.

by Cheremisinoff and Davis (1979) for the fluid mechanics. Dimensionless velocity and distance, u^+ and y^+, are

$$u^+ = u/u^*, \tag{10}$$

where

$$u^* = (\tau_{WL}/\rho_L)^{1/2} \tag{11}$$

and

$$y^+ = yu^*/\nu_L \tag{12}$$

Further, the dimensionless temperature T^+ is defined by

$$T^+ = C_L(T_W - T)\rho_L u^*/q_W, \tag{13}$$

where T_W is the tube wall temperature, which can be a function of angle θ, T is the temperature at distance y, and q_W is the heat flux at the tube wall. Introducing the dimensionless variables, Equation (9) becomes

$$\frac{q}{q_W} = \left(\frac{1}{Pr_L} + \frac{\epsilon_M}{\nu_L Pr_t}\right)\frac{dT^+}{dy^+} \tag{14}$$

Setting $Pr_t = 1$ and making the approximation $q/q_W \approx 1$ as in the case of the shear stress ($\tau/\tau_{WL} \approx 1$), the governing equation becomes

$$1 = \left(\frac{1}{Pr_L} + \frac{\epsilon_M}{\nu_L}\right)\frac{dT^+}{dy^+} \tag{15}$$

The approximation $q/q_W \approx 1$ cannot be expected to be valid for large values of the holdup, R_L, because the cross-sectional area for heat flow varies with the distance from the wall, but we shall apply the approximation over the whole range of R_L encountered in our experiments ($0.02 < R_L < 0.22$). We consider q_W to be constant, which corresponds to the constant wall heat flux experiments described below.

For the laminar sublayer and buffer zone, $0 \leq y^+ \leq 20$, application of Deissler's (1952) expression for ϵ_M gives

$$1 = \left[\frac{1}{Pr_L} + n^2u^+y^+\left(1 - e^{-n^2u^+y^+}\right)\right]\frac{dT^+}{dy^+} \tag{16}$$

where $n = 0.1$. For $y^+ > 20$, application of the von Karman (1939) expression for the eddy viscosity in the turbulent core gives

$$1 = \chi\frac{(du^+/dy^+)^3}{(d^2u^+/dy^{+2})^2}\frac{dT^+}{dy^+} \tag{17}$$

where $\chi = 0.36$.

Using the velocity distribution obtained by Cheremisinoff and Davis (1979), Equation (16) has been integrated numerically to give T^+ as a function of y^+, and Equation (17) can be integrated analytically to give

$$T^+ = T_{20}{}^+ + \frac{1}{\chi}\ln(y^+/20), \tag{18}$$

where $T_{20}{}^+$ is the temperature at $y^+ = 20$ obtained from the integration of Equation (16). The bulk or mixing-cup temperature is defined by

$$T_b - T_0 = \frac{\int_0^{\gamma/2}\int_0^{y_i} u(T - T_0)(R - y)dyd\theta}{\int_0^{\gamma/2}\int_0^{y_i} u(R - y)dyd\theta}, \tag{19}$$

where T_0 is a reference temperature, which for convenience is taken as the local wall temperature, T_W, assumed uniform along the periphery of the tube wetted by the liquid. The upper limit, y_i, is the position of the gas-liquid interface measured from the wall, which is given by

$$y_i/R = 1 - \cos(\gamma/2)(1 + \tan\theta)^{1/2}, \tag{20}$$

and

$$\theta = \cos^{-1}\left(\frac{R - y_0}{R - y_i}\right) \tag{21}$$

In dimensionless form, Equation (19) becomes

$$T_b{}^+ = \frac{\int_0^{\gamma/2}\int_0^{y_i{}^+} u^+T^+(1 - y^+/R^+)dy^+d\theta}{(W^+/2)} \tag{22}$$

where W^+ is the dimensionless flow rate defined by

$$W^+ = 2\int_0^{\gamma/2}\int_0^{y_i{}^+} u^+(1 - y^+/R^+)dy^+d\theta \tag{23}$$

and

$$R^+ = Ru^*/\nu_L \tag{24}$$

Defining a heat transfer coefficient by

$$h_L = q_W/(T_W - T_b), \tag{25}$$

which can be written as

$$h_L = C_L\rho_L u^*/T_b{}^+, \tag{26}$$

the Nusselt number for heat transfer to the liquid phase becomes

$$Nu_L = \frac{h_L y_0}{k_L} = \frac{Pr_L y_0{}^+}{T_b{}^+} \tag{27}$$

where Pr_L is the Prandtl number of the liquid, and $y_0{}^+$ is given by

$$y_0{}^+ = y_0u^*/\nu_L. \tag{28}$$

GAS PHASE HEAT TRANSFER

In the fluid mechanics analysis of Cheremisinoff and Davis (1979), the gas phase pressure drop can be predicted reasonably well by treating the gas flow as if it were single phase flow in a duct of irregular shape, using appropriate friction factors for the wall and interfacial stresses. It is assumed that heat transfer to the gas phase can be treated approximately in the same way, but the model is less appropriate for heat transfer than for pressure drop, for reasons that are discussed below. Since most of the heat is transferred to the liquid phase, except when very small values of holdup are encountered, errors associated with the prediction of the heat transfer to the gas phase do not greatly affect the calculation of the total heat transfer to the two-phase flow.

For single phase flow the Dittus-Boelter equation,

$$Nu_G = 0.023Re_G{}^{0.8}Pr_G{}^{0.4} \tag{29}$$

and the modified Dittus-Boelter equation

$$Nu_G = 0.022Re_G{}^{0.8}Pr_G{}^{0.6} \tag{30}$$

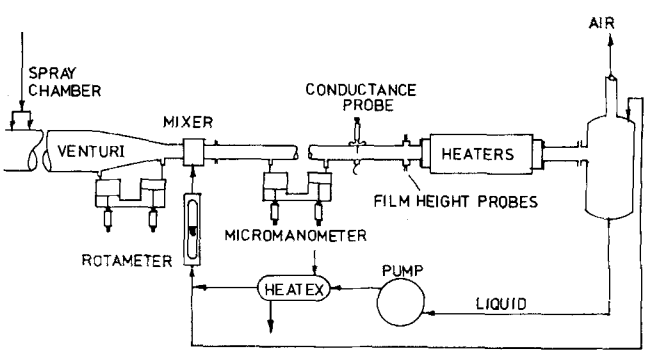

Figure 2. The fluid flow and heat transfer test loop.

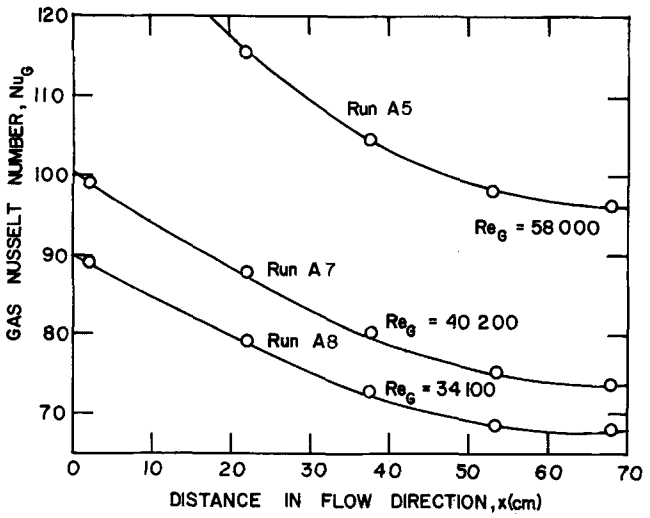

Figure 3. Local Nusselt numbers for air flow as a function of the axial position.

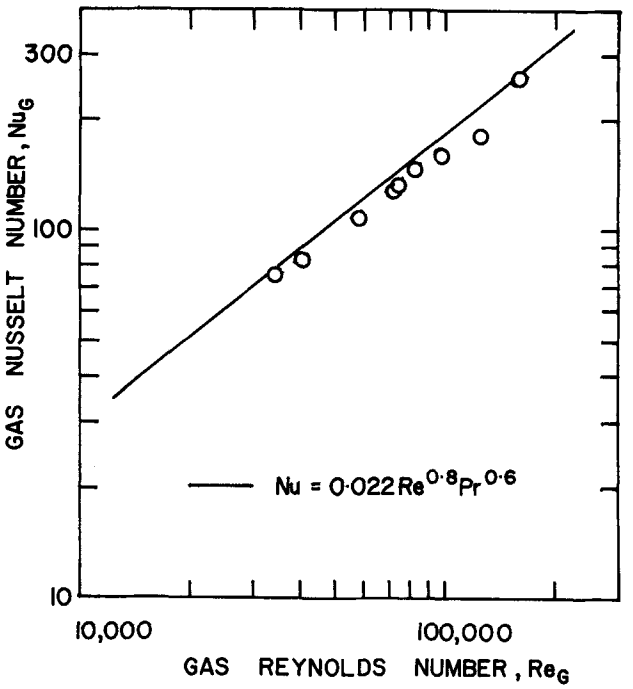

Figure 4. A comparison between the Nusselt numbers for single phase air flow and Equation (30).

have been used to predict heat transfer coefficients. We shall apply these equations to the gas phase, defining the gas Reynolds number by

$$Re_G = D_{EG}\overline{U}_G/\nu_G \tag{31}$$

and the Nusselt number is

$$Nu_G = h_G D_{EG}/k_G \tag{32}$$

where D_{EG} is given by Equation (8), $\overline{U}_G = Q_G/A_G$ and Q_G is the volumetric flow rate of the gas.

TABLE 1. A TABULATION OF EXPERIMENTAL RESULTS

Run	W^+	Re_G	Re_L	y_0/D	R_L	$\overline{q}$ (J^0/m^2-s)	$\Delta P/L$ (N/m^3)	$\overline{Nu}_L$	$\overline{Nu}_G$	D_{EG} (mm)	Interfacial description
1	2,620	34,500	6,530	0.152	0.096	16,650	34.3	13.9	56.3	58.8	RW
2	2,130	36,390	6,210	0.113	0.062	14,990	19.0	9.3	83.4	60.2	SA
3	2,830	28,390	11,990	0.054	0.021	14,170	22.0	4.2	41.3	62.1	TR
4	2,250	25,940	6,320	0.121	0.069	12,180	18.5	8.7	74.5	59.9	SA
5	2,160	39,040	7,270	0.085	0.041	12,200	42.5	8.5	98.9	61.2	TR
6	3,540	30,720	9,250	0.139	0.085	13,580	33.0	15.4	66.3	59.1	TR
7	3,490	44,070	10,870	0.100	0.052	13,590	62.3	14.4	61.7	60.7	EN
8	2,670	36,550	7,440	0.123	0.070	13,610	41.1	12.9	84.0	59.8	RW
9	4,850	18,650	10,590	0.195	0.138	14,920	16.7	15.5	56.1	56.6	SA
10	4,830	29,200	11,350	0.171	0.113	14,930	33.9	18.8	89.1	57.8	RW
11	4,820	43,970	13,400	0.124	0.071	14,930	69.5	19.9	148.2	59.8	EN
12	4,320	25,150	9,900	0.179	0.121	14,930	24.0	15.8	70.3	57.4	SA
13	4,270	33,770	10,940	0.145	0.090	14,930	41.3	18.0	107.4	58.9	RW
14	3,940	28,440	9,760	0.155	0.099	18,330	26.8	14.4	82.1	58.5	TR
15	3,970	42,220	11,260	0.119	0.067	18,340	58.9	17.3	137.0	59.9	EN
16	5,940	39,340	14,500	0.149	0.093	18,340	62.9	24.7	116.9	58.7	EN
17	6,850	31,800	15,620	0.180	0.123	20,250	48.8	25.1	80.7	57.3	RW
18	9,540	28,670	17,490	0.269	0.217	19,520	44.7	35.7	36.6	52.8	RW
19	9,470	39,310	20,250	0.203	0.146	19,520	62.3	33.3	61.4	56.2	RW
20	8,670	54,990	20,080	0.175	0.118	19,520	80.9	32.0	118.2	57.6	EN
21	8,100	54,360	20,370	0.150	0.094	19,520	108.5	25.7	85.0	58.7	EN
22	7,170	37,630	16,260	0.182	0.124	19,520	109.9	25.4	96.6	57.3	RW
23	2,450	22,910	6,500	0.135	0.081	18,190	16.0	8.9	66.2	59.3	SA
24	3,150	23,490	7,780	0.155	0.099	18,410	15.2	11.1	58.6	58.4	SA
25	3,120	31,500	8,540	0.127	0.074	18,410	25.9	12.9	77.1	59.6	SA
26	2,510	36,520	7,380	0.111	0.061	18,400	34.7	10.8	98.1	60.2	TR
27	6,850	35,230	15,510	0.183	0.125	18,420	47.4	25.4	92.9	57.2	EN
28	10,140	86,580	18,490	0.271	0.220	20,250	43.7	34.8	164.8	52.7	EN
29	9,870	35,370	20,090	0.223	0.166	20,260	72.3	39.1	82.0	55.3	RW
30	7,460	35,490	16,560	0.190	0.132	20,250	69.0	25.5	82.2	56.9	RW

Key: SA = small-amplitude waves
TR = transition
RW = roll waves
EN = entrainment

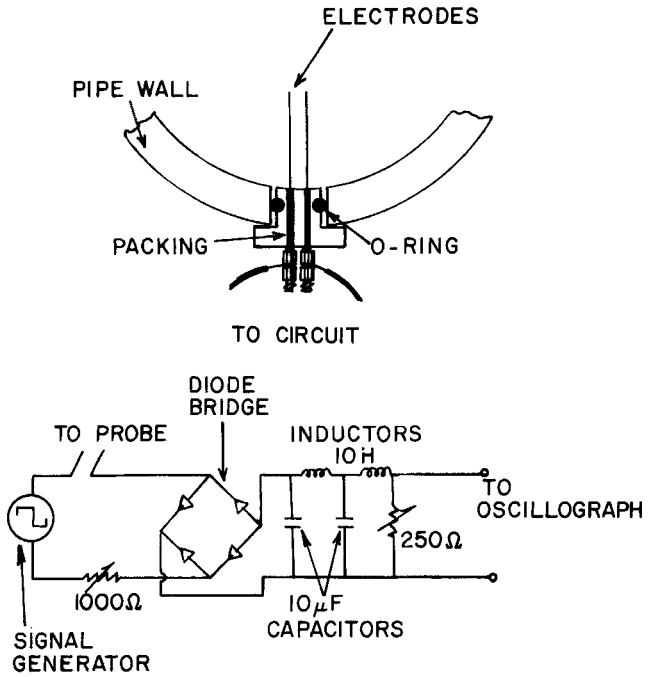

Figure 5. The two-wire conductance probe.

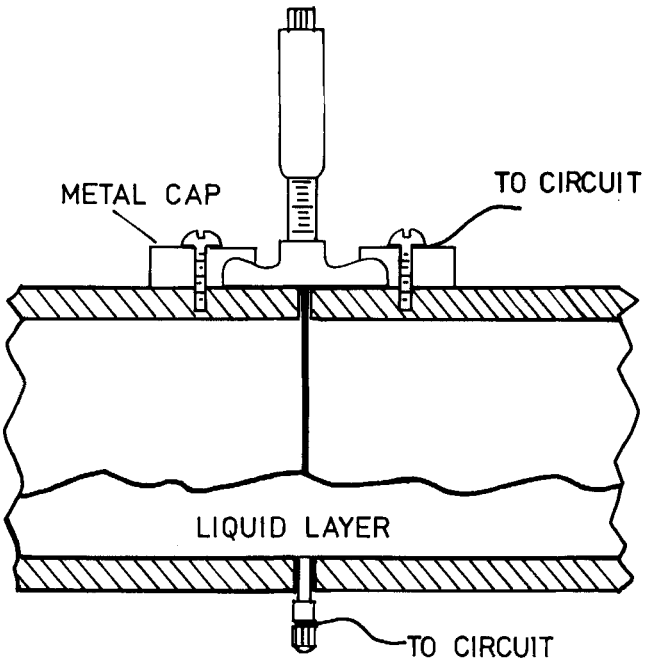

Figure 6. The micrometer conductance probe.

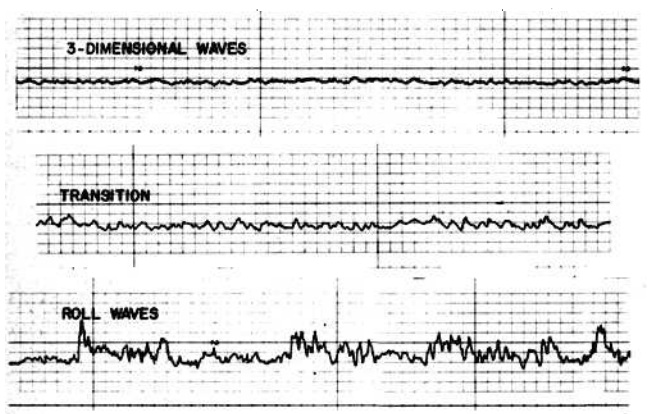

Figure 7. Oscillograph tracings of various interfacial profiles obtained from the two-wire probes.

EXPERIMENTS

Simultaneous measurements of the fluid flow and heat transfer characteristics of stratified air/water flow were made in the test section shown in Figure 2. Details of the flow measurements, wave structure and fluid mechanics parameters were presented by Cheremisinoff and Davis (1979), so we concentrate on the heat transfer measurements here. To the flow loop we added a heat transfer section consisting of a 63.5 mm I.D. aluminum tube of 1.0 m length. The pipe wall thickness was 13.0 mm, and 50 thermocouples were embedded in the wall at various axial, radial and peripheral positions, using the slot and plug design of Pletcher and McManus (1968). Additional thermocouples were installed to estimate heat losses.

The heat transfer tube was wound with nichrome wire at a uniform pitch to provide a constant wall heat flux, and the heater wire is connected as six separate coils, each connected to a powerstat, an ammeter and a voltmeter.

The heat transfer system is tested using single phase air flow over the range of Reynolds numbers encountered in the two-phase flow experiments. Figure 3 shows typical results for the Nusselt number as a function of axial position for various values of Re_G. Asymptotic Nusselt numbers were attained in the downstream half of the test section, and these asymptotic values of Nu_G are compared with Equation (30) in Figure 4. The single phase flow data are seen to be in excellent agreement with the modified Dittus-Boelter equation, the average absolute deviation between predicted and experimental Nusselt numbers being 8.8%.

Thirty experiments involving air/water stratified flow were conducted, covering the range of conditions shown in Table 1. The fluid flow parameters were measured in the manner discussed by Cheremisinoff and Davis (1979). Of particular significance here is the position of the gas-liquid interface, and Figure 5 shows the design of the conductance probes used to measure y_0 and the wave characteristics. A micrometer conductance probe, shown in Figure 6, was used to obtain an independent measurement of the average position of the interface. Typical oscillograph tracings of the output of the two-wire probes are shown in Figure 7. Small-amplitude waves occur at the lower gas and liquid Reynolds numbers, but at higher Reynolds numbers roll waves predominate. At yet higher gas flow rates, droplets detach from the wave crests, and significant entrainment is encountered. Heat transfer data were taken for all types of interfacial conditions up to the point of significant entrainment.

Because the flow loop, except for the heat transfer section, was plexiglas, the interfacial structure could be observed through a flow visualization section consisting of a rectangular box mounted around the circular tube. The space between the box and the tube was filled with the liquid phase to provide an undistorted view of the gas-liquid flow.

EXPERIMENTAL RESULTS

A summary of experimental results is given in Table 1. The Nusselt number, $\overline{Nu}_L$, reported is the average for the liquid phase. Representative circumferential wall temperature distributions for stratified air/water flow are shown in Figure 8. For the portion of the wall in contact with the liquid, wall temperature, T_{WL}, is nearly independent of circumferential position, but large variations in wall temperature occur in the region in contact with

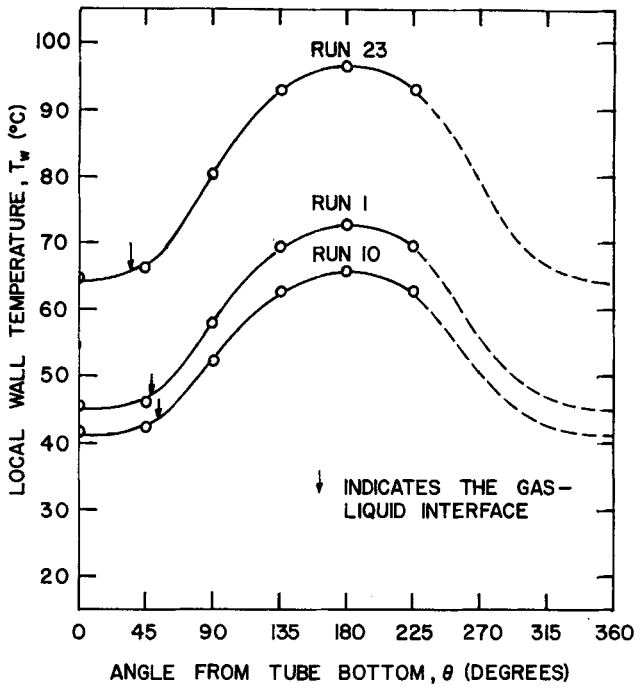

Figure 8. Circumferential wall temperature distributions for stratified air/water flow.

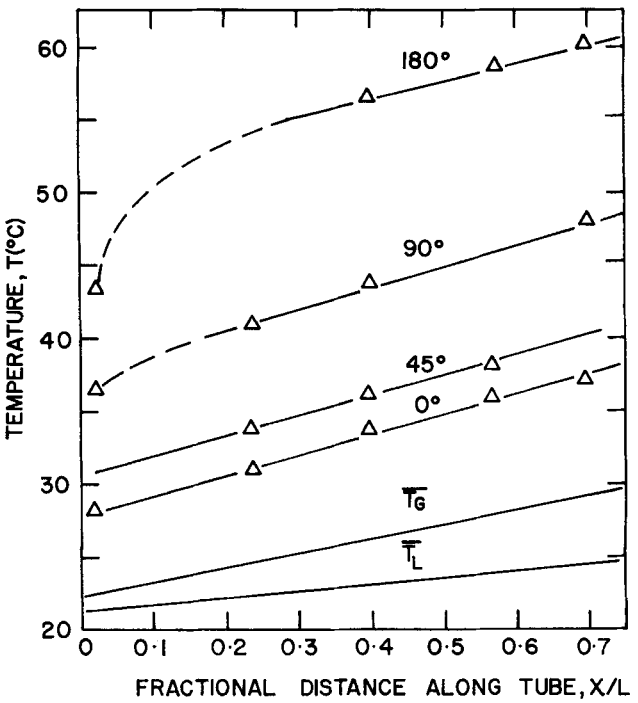

Figure 9. Typical axial temperature distributions.

the gas phase. The lower wall temperatures in the gas phase region near the interface suggest that wave action and droplet deposition cause cooling of the wall, and this effect is substantially reduced as the angle approaches 180° from the bottom of the tube.

Axial variations in temperature are shown in Figure 9, and Figure 10 shows local heat transfer coefficients as a function of circumferential and axial positions. Heat transfer coefficients for the liquid phase are an order of magnitude larger than for the gas phase, and the gas phase heat transfer coefficients vary appreciably with circumferential position due to droplet deposition and wave action near the gas-liquid interface.

The asymptotic Nusselt numbers obtained from the data for the liquid phase are compared with the results predicted from the heat transfer-momentum transfer analogy outlined above, and the results are shown in Figure 11. Experimental values of the holdup are used to determine the geometric parameter γ, which appears in Equations (22) and (23). Agreement between predicted and ex-

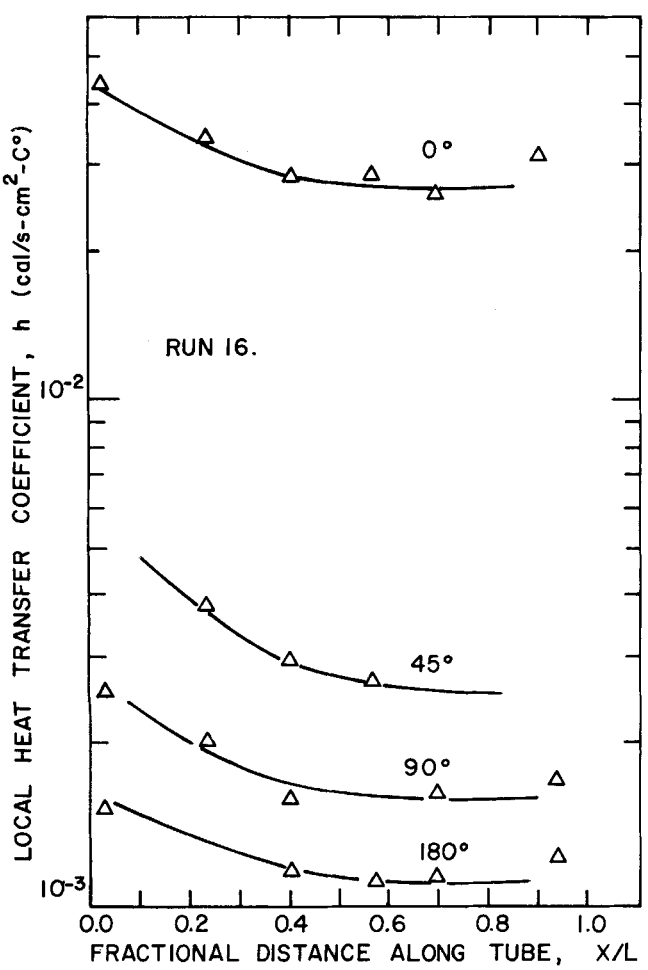

Figure 10. Local heat transfer coefficients as a function of axial position for various circumferential positions.

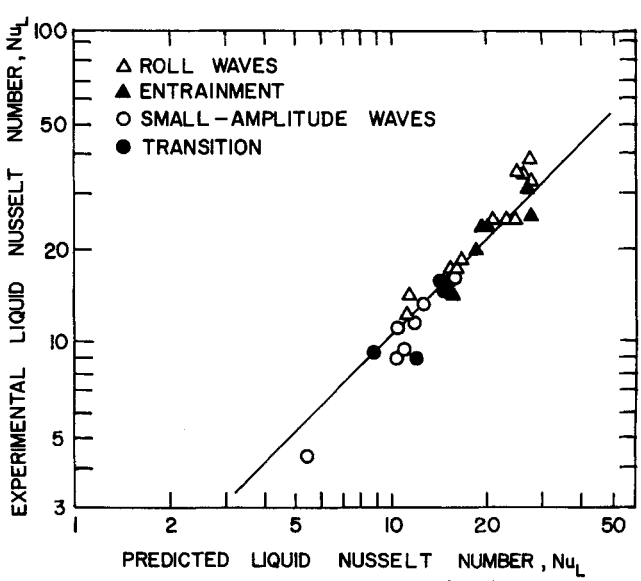

Figure 11. A comparison between measured liquid phase Nusselt numbers and values predicted using the experimental values of the liquid holdup.

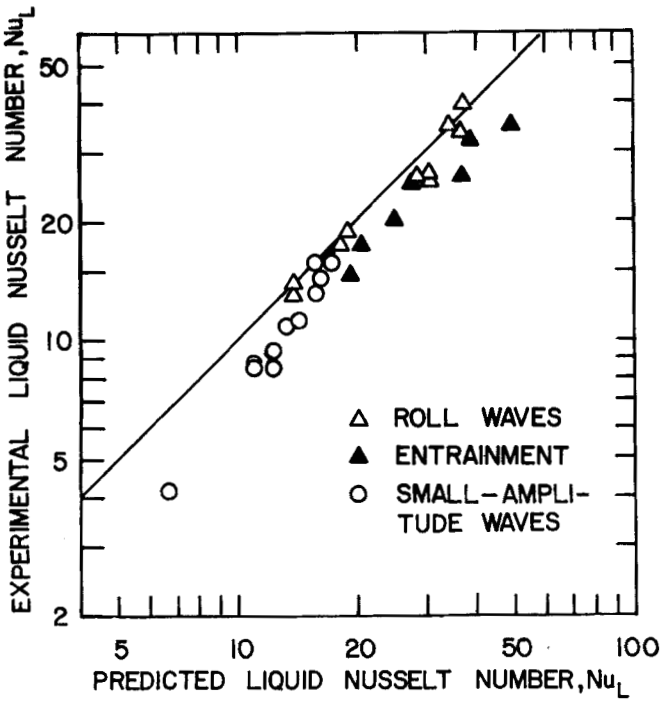

Figure 12. A comparison between measured liquid phase Nusselt numbers and values predicted using the method of Cheremisinoff and Davis (1979) to obtain the liquid holdup.

perimental values of Nu_L is very good, even when some entrainment occurs. The amount of liquid entrained as droplets in the gas phase has not been taken into account, so good agreement between analysis and experiments should not be expected when the amount of liquid entrained is large.

When the method of Cheremisinoff and Davis (1979) is used to predict the holdup, the predicted values of Nu_L are still in good agreement with the experimental values, as shown in Figure 12, but there is a tendency to overpredict Nu_L. The average absolute deviation of the predicted values is 18.7%, using the predicted values of R_L, and using measured values of the holdup the average

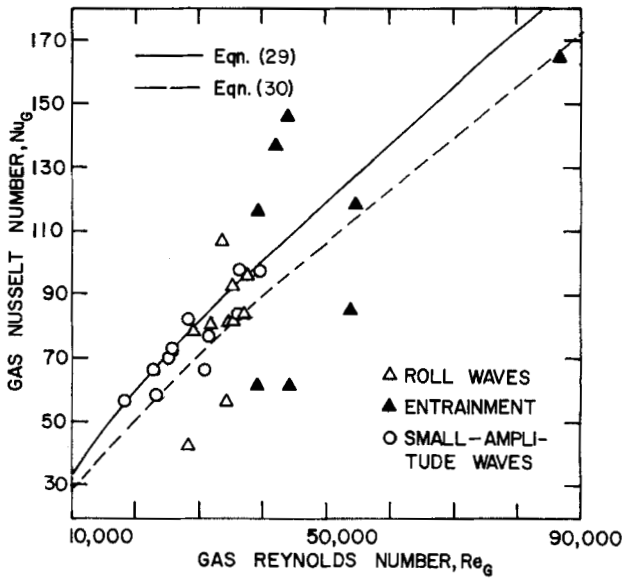

Figure 13. A comparison among measured gas phase Nusselt numbers and Equations (29) and (30).

absolute deviation is 13.0% for the thirty runs plotted in Figure 11.

The prediction of the heat transfer characteristics of the gas phase is less rigorous than that for the liquid phase because of the difficulty associated with taking into account the circumferential variations in Nusselt number due to splashing and droplet deposition, but we have attempted to correlate the average Nusselt number for the gas phase by conventional heat transfer correlations. The circumferential average Nusselt number, $\overline{Nu_G}$, is defined by

$$\overline{Nu_G} = \frac{1}{(\pi - \gamma/2)} \int_{\gamma/2}^{\pi} Nu_G(\theta)\, d\theta \qquad (33)$$

where the integration is over the perimeter in contact with the gas phase. The integration was performed numerically using the experimental data for Nu_G as a function of θ. The results are compared with Nu_G calculated

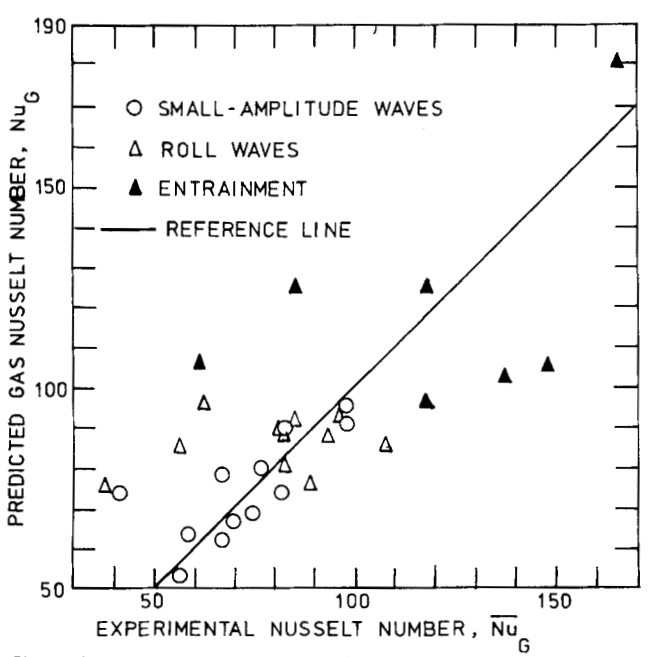

Figure 14. A comparison between the measured average gas phase Nusselt number and Equation (29).

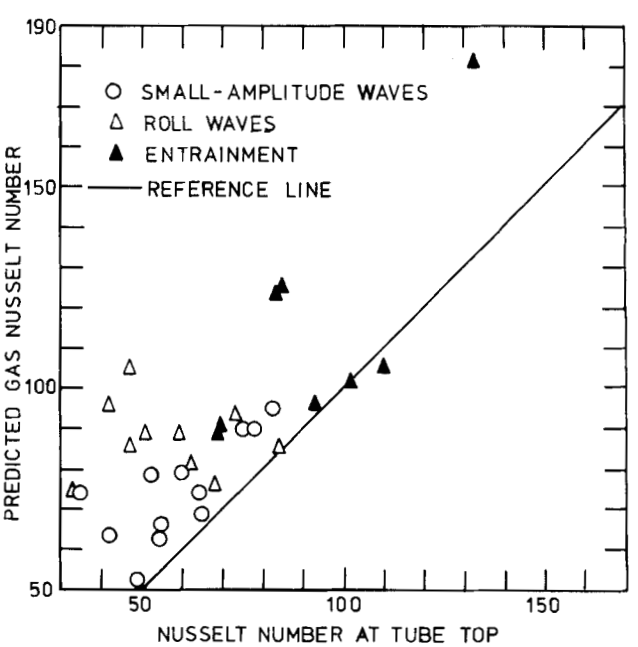

Figure 15. A comparison between the local gas phase Nusselt number measured at the top of the tube and Equation (29).

from Equations (29) and (30) in Figure 13. Although the scatter is large, particularly for roll wave and entrainment conditions, there is reasonably good agreement between the data and Equation (29) for small-amplitude wave conditions. Taking all data points into account, the average absolute deviation between the data and Equation (29) is 21.8% and 21.2% for Equation (30). The results for small-amplitude waves show an average absolute deviation of only 13.6% compared with Equation (29).

It should be pointed out that the Nusselt numbers plotted in Figure 13 are based on the equivalent diameter, D_{EG}, calculated from the measured position of the gas-liquid interface using Equation (8).

Since splashing and droplet deposition on the wall tend to increase the heat transfer coefficient, the magnitude of these effects can be estimated by comparing the average Nusselt number, $\overline{Nu_G}$, with the local Nusselt number measured at the top of the tube where these effects are minimal. Figures 14 and 15 provide such a comparison. The former shows that Equation (29) predicts results which scatter around the data for the average Nusselt number, and the latter shows that the data for Nu_G at $\theta = \pi$ are considerably below the predictions of Equation (29). A comparison between Figures 14 and 15 suggests that splashing and droplet deposition increase the average heat transfer coefficient by about 20% over that expected for a dry wall.

DISCUSSION OF RESULTS

The agreement between the experimental results for Nu_L and those predicted using the analogy between heat transfer and momentum transfer is somewhat better than might be expected, particularly for large-amplitude wave conditions. This is so because the wave action could be expected to increase the turbulence intensity in the liquid layer compared with the turbulence encountered with full tube flow of the liquid phase for the same wall shear. Further, the large-amplitude waves make it difficult to model the liquid layer realistically. Because the mathematical model of the liquid layer and experiments show reasonably good agreement, it can be concluded that wave action does not appreciably alter the transport processes in the laminar sublayer and buffer zone near the wall which comprise the major resistance to heat transfer. It is likely that the temperature and flow fields in the turbulent core of the liquid layer are affected by the waves generated at the gas-liquid interface, but the Nusselt numbers are not greatly enhanced by the waves.

The success of the heat transfer analogy depends on reliable calculation of the fluid flow parameters, particularly the wall shear stress and the holdup. Since these parameters can be predicted for stratified gas-liquid flow by the methods outlined by Cheremisinoff and Davis (1979), their analysis together with the analogy developed here can be used to predict both the flow and the heat transfer characteristics of stratified flows when both gas and liquid phases are turbulent.

ACKNOWLEDGMENT

The authors acknowledge the support of this research by the American Institute of Chemical Engineers through the Design Institute for Multiphase Processing.

NOTATION

A = cross sectional area of the tube, m^2
C = specific heat, J/kg-K
D = tube diameter
D_{EG}, D_{EL} = equivalent diameters for gas and liquid flow cross sections, respectively, m
h = heat transfer coefficient, J/m^2-s-K
k = thermal conductivity, J/m-s-K
n = constant in Equation (16)
Nu = Nusselt number, dimensionless
p_G, p_L = wetted perimeters for gas and liquid phases, respectively, m
Pr = Prandtl number, dimensionless
$Pr_t = \epsilon_M/\epsilon_H$ = turbulent Prandtl number, dimensionless
q = heat flux, J/m^2-s
Q = volumetric flow rate, m^3/s
R = tube radius, m
$R^+ = Ru^*/\nu$ = dimensionless tube radius
R_G, R_L = gas and liquid holdups, respectively
Re = Reynolds number, dimensionless
T = temperature, K
$T^+ = C_L(T_W - T)\rho_L u^*/q_W$ = dimensionless temperature
u = fluid velocity, m/s
$u^* = (\tau_{WL}/\rho_L)^{1/2}$ = friction velocity, m/s
$\overline{U}_G = Q_G/A_G$ = average gas velocity, m/s
w_i = width of the interface, m
W^+ = dimensionless liquid flow rate
y = distance from the wall along the inward normal, m
y_i = distance to the gas-liquid interface, m
y_0 = maximum depth of the liquid layer, m
$y^+ = yu^*/\nu$ = dimensionless distance

Greek Letters

$\alpha = kC/\rho$ = thermal diffusivity, m^2/s
γ = angle subtended by the liquid-wetted periphery
ϵ_H = eddy thermal diffusivity, m^2/s
ϵ_M = eddy viscosity, m^2/s
θ = angle from pipe bottom
μ = viscosity, N-s/m^2
$\nu = \mu/\rho$ = kinematic viscosity, m^2/s
ρ = density, kg/m^3
τ = shear stress, N/m^2
χ = constant in Equation (17)

Subscripts

b = refers to the bulk liquid
G = refers to the gas phase
i = refers to the gas-liquid interface
L = refers to the liquid phase
0 = refers to the tube bottom
W = refers to the wall

LITERATURE CITED

Agarwal, S. S., G. A. Gregory, and G. W. Govier, "An Analysis of Horizontal Stratified Flow in Pipes," *Can. J. Chem. Eng.*, 51, 280 (1973).

Cheremisinoff, N. P. and E. J. Davis, "Stratified Turbulent/Turbulent Gas-Liquid Flow," *AIChE J.*, 25, 48 (1979).

Davis, E. J., S. C. Hung and S. Arciero, "An Analogy for Heat Transfer with Horizontal Stratified Gas-Liquid Flow," *AIChE J.*, 21, 872 (1975).

Davis, E. J., N. P. Cheremisinoff and G. Sambasivan, "Heat and Momentum Transfer Analogies for Two-Phase Stratified and Annular Flows," in *Two-Phase Transport and Reactor Safety, Vol. II*, T. N. Veziroglu and S. Kakaç, eds., Hemisphere Press, pp. 577-608 (1977).

Deissler, R. E., "Analytical and Experimental Investigation of Adiabatic Turbulent Flow in Smooth Tubes," NACA-TN-2138 (1952).

Dukler, A. E., "Fluid Mechanics and Heat Transfer in Falling Film Systems," ASME-AIChE 3rd National Heat Transfer

Conference (1959) and *Chem. Eng. Prog. Symp. Series*, 56, No. 30, 1 (1960).
Etchells, A. W., "Stratified Horizontal Two-Phase Flow in Pipes," Ph.D. Thesis, University of Delaware (1970).
Govier, G. W. and A. Aziz, *The Flow of Complex Mixtures in Pipes*, pp. 500-625, Van Nostrand-Reinhold, New York (1972).
Hewitt, G. F., "Analysis of Annular Two-Phase Flow, Application of the Dukler Analysis to Vertical Upward Flow in a Tube," AERE-R 3680, H.M.S.O. (1961).
Pletcher, R. H. and H. N. McManus, "Heat Transfer and Pressure Drop in Horizontal Annular Two-Phase, Two-Component Flow," *Int. J. Heat Mass Transfer*, 11, 1087 (1968).
Rosson, H. F. and J. A. Myers, "Point Values of Condensing Film Coefficients Inside a Horizontal Pipe," *Chem. Eng. Prog. Symp. Series*, 61 (59), 190 (1965).
Russell, T. W. F., A. W. Etchells, R. H. Jensen and P. J. Arruda, "Pressure Drop and Holdup in Stratified Gas-Liquid Flow," *AIChE J.*, 20, 664 (1974).
von Karman, T., "The Analogy between Fluid Friction and Heat Transfer," *Trans. ASME*, 61, 705 (1939).
Yu, H. S. and E. M. Sparrow, "Stratified Laminar Flow in Ducts of Arbitrary Shape," *AIChE J.*, 13, 10 (1967).

Manuscript received February 24, 1978; revision received June 4, and accepted June 18, 1979.

Diffusivities of Low-Volatility Species in Light Gases

PERIASAMY RAVINDRAN
E. J. DAVIS
and
A. K. RAY

Department of Chemical and Nuclear Engineering
University of New Mexico
Albuquerque, NM 87131

Gas-phase diffusivities for high boiling point organics in common gases are determined by evaporating a single submicron aerosol droplet of the organic species, while it is suspended in an electric field in the path of a polarized laser beam. The droplet size is measured as a function of time by using Mie theory to determine the size from the light scattering data of intensity versus angle. In addition to diffusivities, the Lennard-Jones molecular interaction potential parameter, ϵ_{ii}, and the collision diameter σ_{ii}, are found, by applying the molecular theory of gases to interpret the evaporation rate data. Results are compared with available empirical and semi-theoretical correlations for diffusivities and Lennard-Jones parameters. The low vapor pressure organics used here are dioctyl phthalate (DOP), dibutyl sebacate (DBS) and dibutyl phthalate (DBP), and the carrier gases are helium, nitrogen and carbon dioxide.

SCOPE

Predictions of mass transfer rates in a wide variety of gas phase chemical processes require knowledge of diffusion coefficients. Furthermore, the prediction of the lifetime of low-volatility aerosol droplets in the atmosphere requires knowledge of their vapor pressure and the diffusivity of their vapor in the surrounding air. As indicated by Fuller et al. (1966), a large amount of data is available on binary gas phase systems of relatively low molecular weight, for example, ethanol in air, nonane in nitrogen, etc. Further, the kinetic theory of gases, as presented by Hirschfelder, Curtiss and Bird (1954), provides a rigorous theoretical method for predicting gas phase diffusivities for systems whose Lennard-Jones molecular interaction parameters are known or can be obtained from viscosity data.

Numerous empirical and semi-theoretical correlations have been proposed for the estimation of diffusivities. Among these are the equations of Arnold (1930), Gilliland (1934), Andrussow (1950), Chen and Othmer (1962) and Fuller et al. (1966). Correlations are available for predicting the Lennard-Jones parameters, and these include the methods of Hirschfelder, Bird and Spotz (1949), Wilke and Lee (1955), Chen and Othmer (1962), Stiel and Thodos (1962) and Viswanath and Kuloor (1967). Recently Reid, Prausnitz and Sherwood (1977) reviewed some of the proposed methods of parameter estimation and compared some of the methods of estimating gas-phase diffusion coefficients.

Most of the correlations have been compared with data for systems involving relatively low molecular weight species with low boiling points in common gases. Data are scarce for large molecular weight species with high

0001-1541-79 3056-0966-$01.15.